ABSTRACT

Satellite imagery-based stereoscopy is fast becoming a worthy substitute for ariel stereoscopy. This is due to modern technological advancement that has seen satellite imagery rivaling Ariel Photography in spatial revolution, extent and overlap necessary for 3D modeling. The purpose of this paper is to create a Digital Surface Model of two divergent study areas (one urban and one rural) using state-of-the-art methods and Satellite imagery. Also, two software are tested to compare efficiency, ease, and accuracy. It is found that neither the Agisoft nor MicMac-created DSMs can be ranked equally with the lidar-derived DSM in terms of noise, vertical and horizontal accuracy, the MicMac DSM fared better than Agisoft in terms of horizontal and vertical accuracy alone (with a height RMSE of 48m against Micmac's 108m), while the Agisoft DSM performed better than MicMac in terms of noise. Also, in terms of usability and efficiency, Agisoft exceeds Micmac significantly due to its straightforward workflows and GUI, documentation, and processing timeline.

1. INTRODUCTION

Digital Surface Models (DSMs) are continuous surface models that represent the elevation values of the Earth's topographic surface, including objects such as buildings, vegetation cover, and natural terrain features. DSMs are a subset of Digital Elevation Models (DEMs), which also include digital terrain models (DTMs) that portray the bare-earth surface. DSMs, being comprehensive and rich models, have gained significant importance in various fields, including remote sensing, GIS, cartography, geophysics, environmental sciences, engineering, and more. Fig 1 illustrates the differences between DSM, SEM, and DTMs.

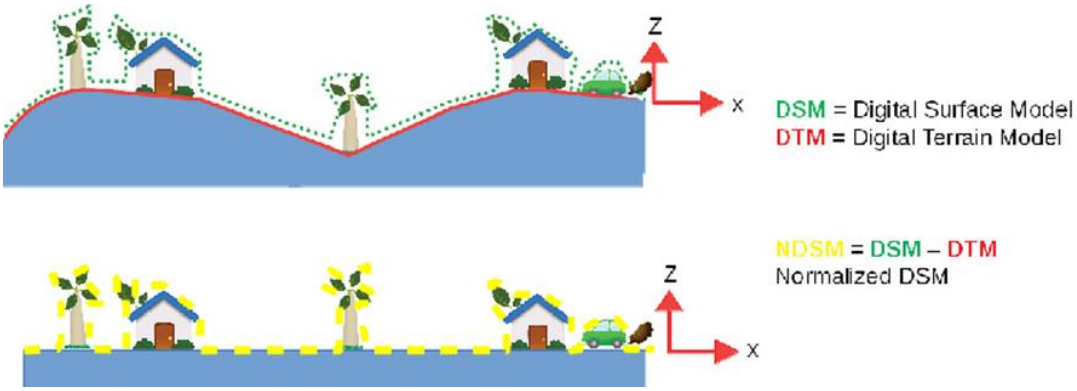

Figure 1. Difference between DSM, DTM, and DEM. (source: UP42)

The uses of DSMs are diverse and essential. They have become essential not only in man's 21st-century quest for digital earth. A virtual twin of the earth whereby autonomous vehicle navigation and the Internet of Things thrive. DSMs and other 3d models of the earth are essential for even more crucial exercises such as flood zone modeling, disaster/hazard management, precision agriculture, maritime navigation, space mission planning environmental studies, and even in medical applications (such as the emerging field of drone-enabled delivery of medical supplies).

Figure 2. DSMs in Flood Modeling/Disaster Management (source Markis et.al. 2023)

DSMs aid in understanding terrain characteristics, allowing researchers to analyze landscapes, conduct 3D simulations of earth processes and also estimate river channels' extent and impact. This is exemplified by (Yang et al., 2011) in their quote "Topography is a basic constraint and boundary condition not only to hydrologic models of flooding and runoff and atmospheric boundary layer friction theories but also to global change and regional sustainable development research".

Exploring, in particular, the importance of DSMs to flood modeling, this paper seeks to compare DSMs created using currently available state-of-the-art methods and software (both proprietary and open source), to evaluate vertical and horizontal accuracy, software efficiency, and ease of use. Finally, the resulting DSM will be tested in a simple 1D flood model to comparatively evaluate performance.

1.1 Motivation for this paper

As a person with a vested interest in the subject matter of Flood modeling, particularly urban flood modeling, for this project, I was particularly inspired by Google Earth's Sea Level Rise and the fate of Coastal Cities product, which represented with striking visuals the potential impact of sea level rise on the topography of coastal cities. While some cities such as London were visualized in stunningly realistic 3D models, that showed the potential extent of the city likely to be permanently flooded in the event of continuous global warming (at 2°c and 4°c) and resulting sea level rise, other cities such as Mumbai and Lagos were not afforded such detail. This coupled with the fact that there are currently no publicly available high-resolution DSMs for any parts of Africa, as of 2023, as confirmed by an extensive search conducted by myself and a few colleagues in the 1st semester, led me to seek out the knowledge of what exactly goes into DSM model creation. This paper will detail my findings in this quest. As a side note, the only currently open-source DSMs for Africa (and globally) are JAXA's 30m DSM which, would not have been able to reproduce the google earth visualization mentioned above, and according to research would perform particularly poorly in urban flood modeling.

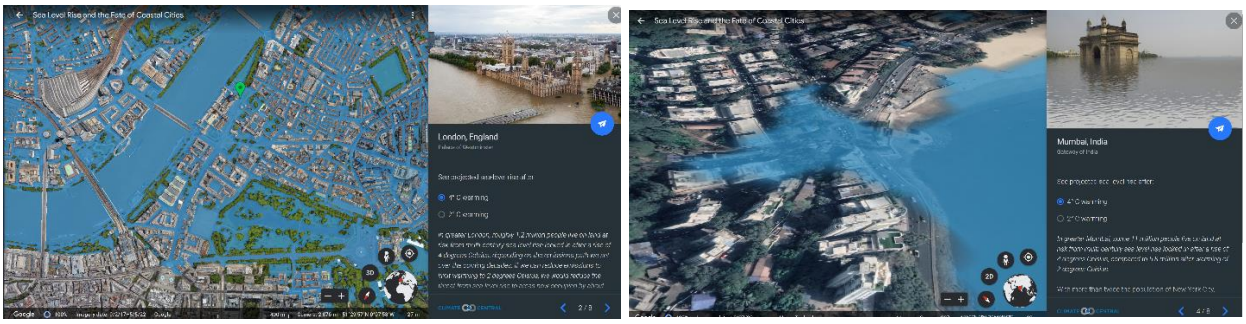

Figure 3. The role of DSM in Flood modeling. Google Earth's Sea Level Rice product. (Source: Googe Earth)

1.2 How DSM accuracy may affect flood model outcomes.

Having established that DSMs provide detailed representations of urban topography, it is important to further establish the link between the use of accurate DSMs in flood models to the accuracy of the resulting flood model. Flooding in urban environments involves complex interactions between surface features, infrastructure, and drainage systems. When DSMs lack accuracy, flood models may fail to capture these intricate processes, resulting in flawed flood risk assessments and inadequate resilience planning.

(Reinstaller et al., 2022) highlights the importance of model uncertainties and calibration in urban flood models [1]. According to them, inaccurate DSMs can lead to improper calibration of model parameters, such as surface roughness, especially in steep peri-urban catchments. Incorrect calibration may result in an inaccurate representation of flow and water depth, leading to unreliable flood predictions.

Furthermore, (Bodoque et al., 2023) emphasize the need for geometrically consistent DSMs in flood hazard mapping [2]. LiDAR data alone may not produce geometrically accurate DSMs, particularly in urban areas with complex geometric features. Inaccurate DSMs can lead to fake water flow barriers and unrealistic representations of the urban domain, affecting the reliability of flood hazard maps. This poses a significant challenge for flood risk management and emergency response planning.

In essence, accurate DSMs are critical for reliable urban flood modeling and the accuracy is largely dependent on the factors surrounding its creation.

1.3 Objectives

The specific objectives of this paper are outlined as follows;

- Using existing tools (open source (MicMac), proprietary (Agisoft Matashape))
- Produce DSMs using available Pleiades Imagery (Salzburg, Shalla Lake)
- Compare results with reference (where available) and method/tool efficiency
- Compare efficiency in terms of
    - Processing Time
    - Backend Processing Transparency
    - Documentation (Ease of Use)
- Build a simple 1d flood model to test its efficiency and difference in accuracy.

2. DATASETS

2.1 Satellite Imagery

Location	Resolution	Land Use Type	Date	Source
Salzburg, Austria	0.50cm Panchromatic, 2m Multispectral	Urban	2015	Pleiades 1A
Shalla Lake, Ethiopia	0.50cm Panchromatic, 2m Multispectral	Rural	2018	Pleiades 1A

Table 1

2 sets of Pleiades stereo triplet files were graciously made available for this study by the staff of the Christian Doppler Laboratory (GEOHUM). Both Imagery sets, each made up of tri-stereo pairs shipped with at-sensor geometric processing and basic radiometric processing. They both possess DIMAP-type metadata files which allowed for an easy-to-use webpage visualization of the metadata.

They also come with the RPC sensor model which is the industry standard that tells of the sensor calibration and serves as a key input for DSM generation.

Significant advantages have been linked to the tri-stereo method applied by Pleiades, which allows 3 images to be captured with a second interval at 3 different angles.

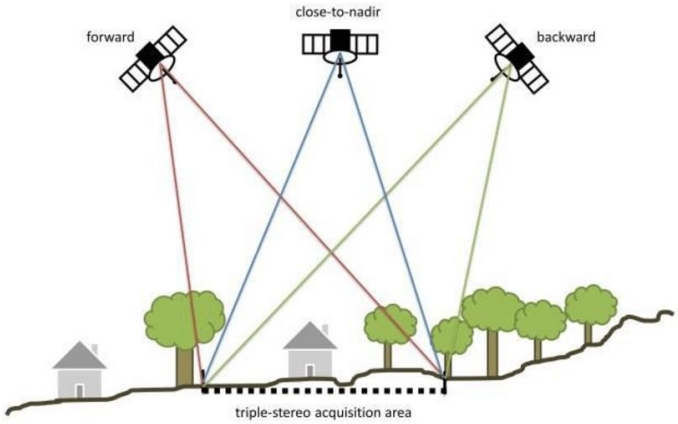

Figure 4. Tri-stereo Satellite imagery acquisition (Source Riedler et al., 2017)

There are several advantages associated with this acquisition mode. Firstly, the Incidence angle is the same for all images in the triplet. Vertical accuracy is largely determined by incidence angle. Research shows that DEM creation is best at incidence angles less than 35 degrees (Gong Ke & Fritsch Dieter, 2019). Also, mixing images of even the same scene but at different incidence angles is proven to lead to significant vertical errors (Palaseanu-Lovejoy et al., 2019).

Another significant advantage is that the RPC model is available, and sensor calibration (Attitude and Ephemeris are precise) is done already. So additional Bundle Adjustment can be skipped. (Palaseanu-Lovejoy et al., 2019). Otherwise, the sensor ephemeris/attitude information needs to be calculated by applying the bundle adjustment algorithm.

2.2 Lidar DSM

Austria 1m DSM: Obtained using the University of Salzburg Department of Geoinformatics WMS. Link. This is the standard DSM for Salzburg created through Lidar scanning and updated every 5 years. The 2019 version is used as the reference in this paper to test the accuracy of the photogrammetry methods and software used. Its CRS is WGS 84 Pseudo Mercator (WKID 3857).

3. METHODOLOGY

There are several methods to create DSMs, and this section highlights three prominent techniques: Lidar, Satellite Stereo Photogrammetry, and Ariel Stereo Photogrammetry.

3.1. Overview

3.1.1 LiDAR (Light Detection and Ranging) is a remote sensing technology that uses laser pulses to measure distances to the Earth's surface. Mounted on aircraft or drones, Lidar systems emit laser beams toward the ground, and the reflected signals are used to derive accurate elevation data points. Lidar is renowned for its high precision, capable of capturing dense point clouds, with each point representing X, Y, and Z coordinates of points on the earth, which can be further interpolated to create detailed DSMs. The most advanced and high-resolution DSMs currently available are created using Lidar. However, Lidar acquisition and processing costs are very high.

3.1.2 Satellite Stereo Photogrammetry (SSP): relies on satellite images of the same area, but taken from different angles to extract 3D information about the Earth's surface. Thanks to the recent advancement in satellite data acquisition offering stereo and even tri-stereo acquisition capabilities, significant overlap is achieved (up to 90% vertical and horizontal) which is crucial for DSM generation. This coupled with the advent of sub-meter resolution satellite imagery (up to 30cm resolution for Airbus's Pleiades Neo) offers a cost-effective and scalable solution for generating DSMs over large areas. This technique, which is similar to ariel photogrammetry offers significant advantages over the latter as its scalability represents significant cost savings.

3.1.3 Ariel Stereo Photogrammetry (ASP) is similar to SSP but involves using images captured from aerial platforms, such as airplanes, helicopters, or drones. Traditionally stereo photogrammetry was ariel stereo photogrammetry with the satellite imagery-based one being a later development. Due to the cost savings from SSP, ariel photogrammetry is now more useful for small-scale DSM generations such as corridor mapping, precision agriculture, etc. where scalability is not a priority.

In this paper, the focus, however, is on Satellite Stereo Photogrammetry. 2 sets of tri-stereo imagery (3 overlapping satellite images of the same areas) are processed using state-of-the-art open-source and proprietary photogrammetry software, and the results compared to a Lidar reference (where available) and also compared in a simple 1D flood model simulation to evaluate performance.

3.2. Standard Satellite Imagery Stereo-Photogrammetry Processing Workflow.

Stereo Photogrammetry is based on the principle of Stereo Matching. Stereo Matching is used for finding corresponding pixels in a pair of images, which allows 3D reconstruction by Triangulation, using well-known intrinsic and extrinsic orientations of the cameras. Note that in conventional ariel stereo photogrammetry, an overlap of between 60% to 80% is recommended wherein only the overlapped region will produce depth (Z values). However, Stereo pairs/triplets obtained from satellite imagery usually possess significantly higher overlaps, up to 90% vertical and horizontal.

Below are the steps usually taken in a standard stereo photogrammetry pipeline. These steps are almost all employed in the 2 different software this research utilized. However, this section serves as an overview of all the steps.

3.2.1. Camera Calibration: Upon loading images into any photogrammetry software, the first point of call is the camera calibration settings where the know camera position and orientation (both internal and external) at the time of image capture/acquisition are imputed (correcting for sensor and acquisition specific errors like jitters in the case of satellite acquisition). Imputing precise values in this step is germane as it impacts the ability of the algorithms in the image alignment and tie point generation steps. Pleiades

product ships with both exact (DIM) and approximate (RPC) sensor models (ASP Docs). The RPC model represents calibrated intrinsic and extrinsic parameters of the sensor. This has been rigorously corrected for sensor-specific errors or artifacts (already corrected Ephemeris and Attitude). But Bundle Adjustment may be used to further optimize this.

3.2.2. Image Alignment: This entails positioning the images in an optimal manner for efficient tie point identification. An alignment process is needed to narrow down the number of image pixels that must be searched through to find correspondences among the two images used in stereo. Technically, it involves the reduction of the y-parallax to 0 (See figures 5 and 6).

Image alignment enables the use of Epipolar Geometry which is a 1D rather than 2D search in the image space for matching points in the object space. in Tie point search (next step). A popular method for doing this in literature is the Popular in literature is Affine Epipolar methods of image alignment, where an affine transformation is applied to both the left and right images to make the epipolar lines approximately horizontal (thus similar).

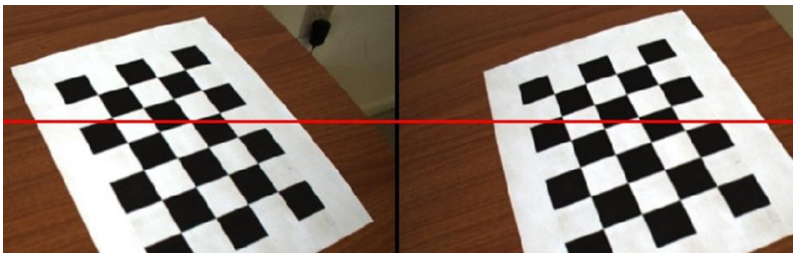

Figure 5. Unaligned images with y parallax noticeable

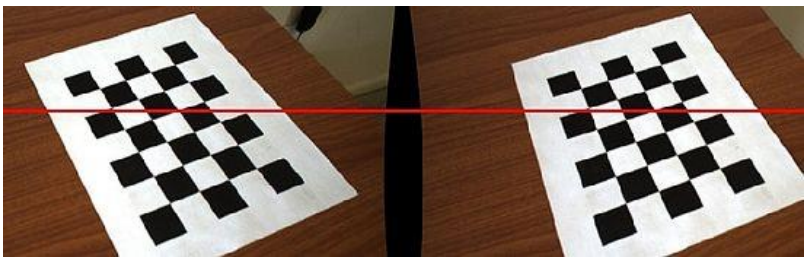

Figure 6. Rectified: epipolar are at infinity along the x-axis, meaning they both have the same y-axis coordinates (Y-parallax is eliminated). This knowledge allows for faster searches during correlation.

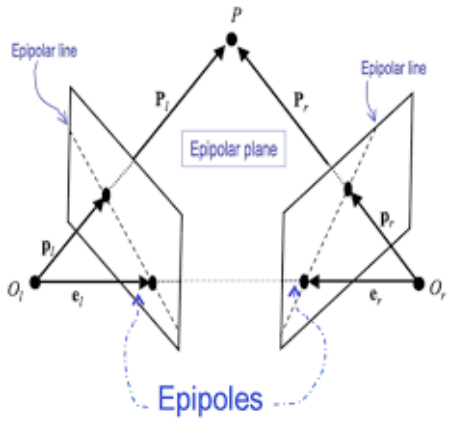

Figure 7. Epipolar Geometry.

A vital method that allows the algorithms responsible for searching the images for tie points to search efficiently in 1D instead of 2D searches like block matching which is usually less detailed and more computationally expensive.

3.2.3. Tie Point Creation: Within the image space, similar points are identified in the overlapping region of the image. A collection of algorithms is run to compute these correspondences between pixels in the left and right images. This results in a disparity map. The resulting points have x and y image coordinates only and no depth (z) values at this point. Popular methods in the literature for this are Semi-Global Matching (SGM), More Global Matching (MGM), etc.

3.2.4. Bundle Adjustment (with or without GCPs): This involves the iterative triangulation on all images (stereo) to ensure minimum error between points measures in the image and on the ground. It utilizes all possible intrinsic and extrinsic parameters to iteratively determine the exact conditions at the time of capture, keeping possible errors to the minimum. This step is optimally done with Ground Control Points (GCPs). As mentioned earlier in this paper, this step can be skipped when using a satellite image pair/triplet which

ships with its thoroughly calibrated and corrected sensor parameters like Pleiades does. It is important to note that this step does not necessarily contribute to the vertical or horizontal accuracy of the resulting DSM, as it only deals with the alignment of the sensor model at the time of image capture.

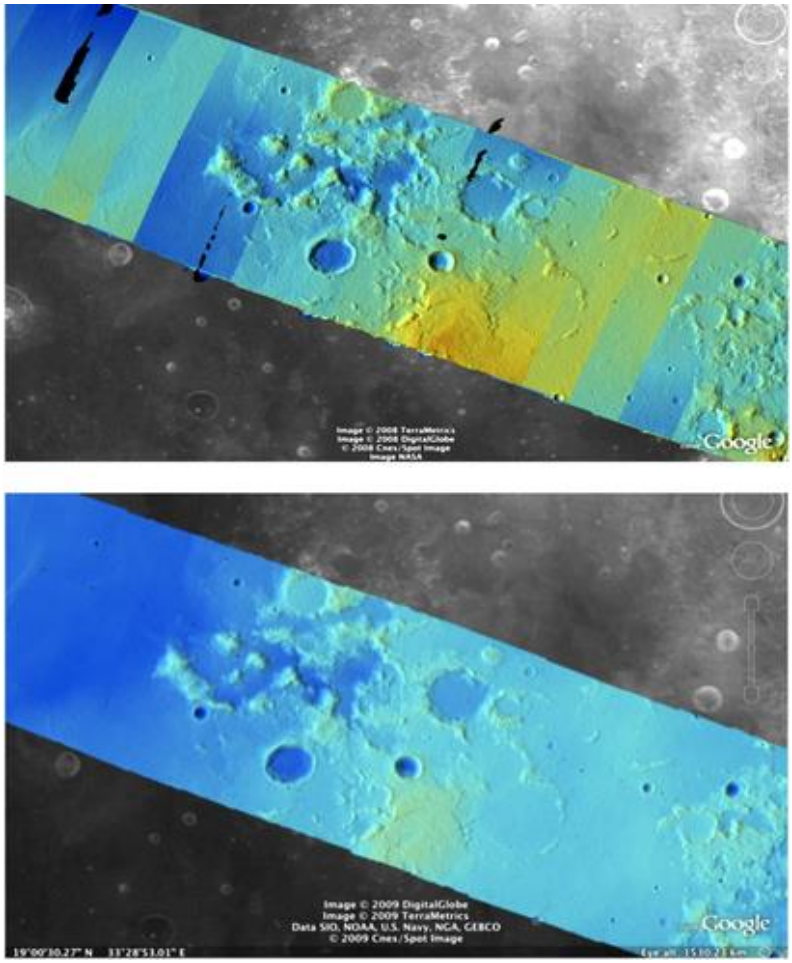

Figure 8. Uncalibrated sensor models before and after BA.

3.2.5. Depth Map Creation/Point Cloud Generation: Through the process of Triangulation, the disparity map is converted to a Depth Map. The depth Map is a 3D image map for which every pixel has an x, y, and z dimension.

3.2.6. Point Cloud is created (points instead of a continuous surface): Similar to tie points but now with x, y, and z values and scaled to real-world coordinates (based on specified project reference system).

3.2.7. DSM Creation and Georeferencing: DSM Creation from Depth Map/Point Cloud: Here interpolation (for point cloud) and georeferencing are done to bring the depth map into real-world coordinates.

3.4. Software-specific processing Workflow

The two software compared in this paper are Agisoft Metashape and Micmac.

3.4.1. Agisoft Metashape Workflow and Peculiarities

This is powerful proprietary photogrammetry software that is popular and widely used among professionals. It is built in C++ and possesses a graphical user interface. It is easily installed with a precompiled version for Windows. It also has an updated and user-friendly user guide and documentation. For this research, a free 30-day trial license was utilized. While it is easy to use with example workflows and tutorials available, including a standard satellite imagery DSM generation pipeline, that came in very handy for this analysis. One major downside is that backend processing steps are not always fully explained in the docs.

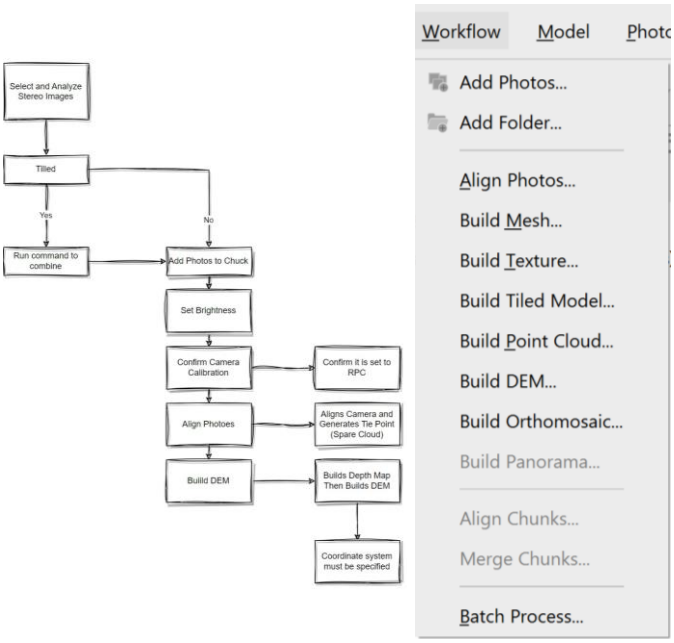

Figure 8 illustrates the workflow followed for this analysis.

3.4.2. Peculiarities that differ from the standard workflow.

a. Camera Calibration is done automatically upon loading satellite imagery into the workflow (add folder). If this is not done, it is advised to confirm that the camera type is set to RPC. Once this is done, the NA (not aligned) flag is removed from them.

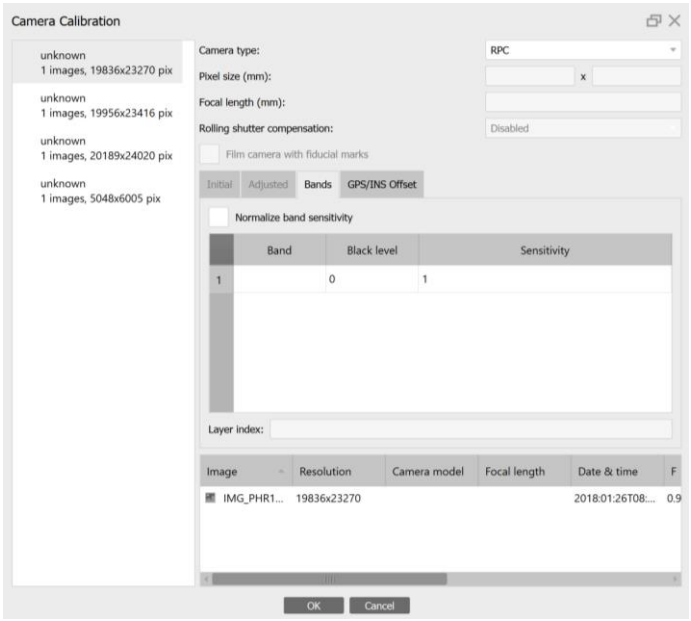

Figure 9. RPC is selected as the camera type in the camera calibration window, showing that the provided RPC file has been accurately identified.

b. Upon image loading, image brightness settings may need to be adjusted for satellite imagery as it initially appears very dark. The “estimate brightness” prompt automatically selects the optimal brightness level for the image.

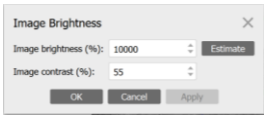

c. Upon Image alignment, tie points are automatically created.

d. Two types of bundle adjustment can be done. One uses exact GCPs while the other does not. Bundle adjustment can be done with GCPs (update transform) if accurate GCPs are provided. However, this step was performed without GCPS by simply clicking the update transform button because of the lack of very accurate GCPs at the moment of analysis.

   According to research, when using RPC-applied satellite imagery, it is better to avoid bundle adjustment than to do it with inaccurate GCPS.

e. Depth maps/Disparity maps may be calculated independently or skipped to create the DEM/DSM directly. If the latter is done, however, the depth map is still created anyway before the DEM can be created.

Figure 10. 3D model of Salzburg showing the orientation of the sensors(cameras) at the time of capture as obtained from the RPC model parameters.

f. As an intermediate step, this 3D model (Mesh) may be derived from the created depth map. The only difference between this and a DSM/DEM is that the latter is georeferenced.

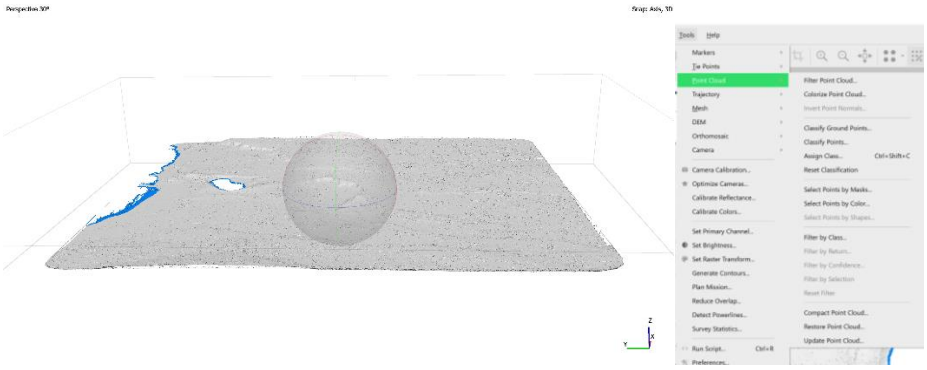

Figure 11.

g. A cleaning step was necessitated for the Shalla Lake analysis as the resulting DEM was flawed due to outliers (particularly over areas with water). Cleaning was done first by generating a point cloud which was then manually classified into water and non-water points. The DSM generation algorithm was then run on the non-water points alone. See the figure below.

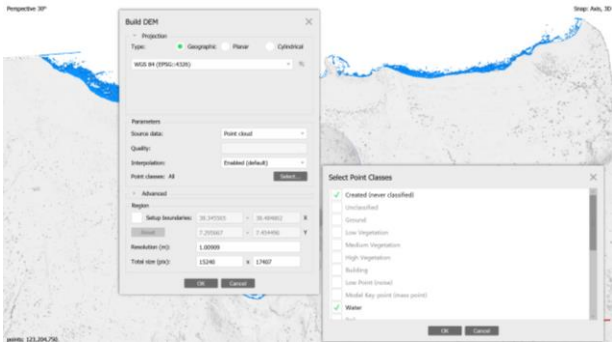

Figure 12.

3.4.3. Micmac DSM: describe workflow and peculiarities

This is a free and open-source alternative to Agisoft Metashape**.** It is a powerful command line tool. It however has a steep learning curve and may be slightly too complicated for absolute beginners. One major downside to it is that it does not hint at recommended

system types and capacity specifications. It also has no means of determining the progress or estimated runtime of steps. It offers numerous tutorials to learn from but very little for satellite image processing. It is however very powerful and capable of yielding reasonable results.

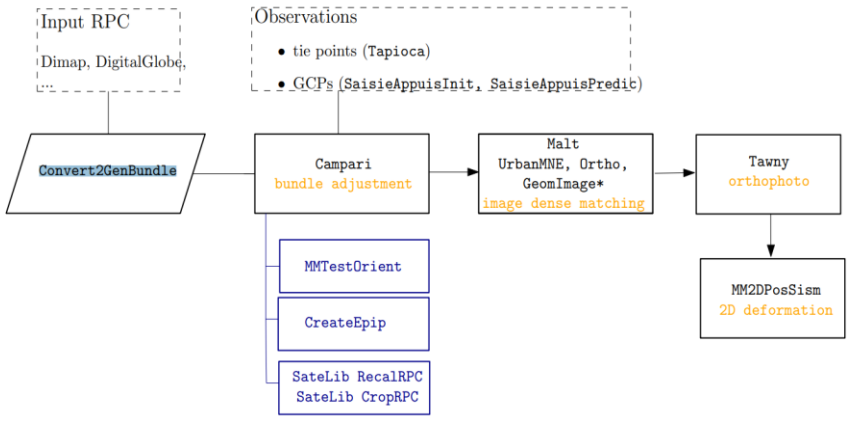

Figure 13. is an illustration of the Micmac processing workflow (Source: Micmac docs)

3.4.4. Peculiarities of Micmac

a. Only .tif imagery files can be processed in Micmac.
b. Tiepoints are generated using the Tapioca algorithm. Please see Micmac documentation for more details on the input parameter options. Although running the algorithm alone without parameters (e.g. mm3d Tapioca) returns a help promptly.

Code

***For full resolution*

mm3d Tapioca All .*tif -1

***To reduce computational time by downsampling the input images, such that the larger dimension (usually the width) is no greater than the pixel count specified e.g. 15000*

mm3d Tapioca All .*tif 15000

c. The input files with rational polynomial coefficients must first be converted to a MicMac readable format, and the processing coordinate system is defined using the

Convert2GenBundle command. The processing coordinate system must be specified in a peculiar .xml format beforehand.

Figure 11. .xml file containing the processing coordinate system.

Code

```
mm3d Convert2GenBundle "(.*).tif" "$1.xml" RPC-d0
ChSys=WGS84toUTM.xml Degre=0
```

d. Regular expressions are heavily used and it is expected that any potential user of Micmac is familiar with them. E.g in the example above, the images (all triplets) are represented using “(.*).tif” while their corresponding RPC files are referred to by “$1.xml”

e. Bundle adjustment is done in 5 iterative steps. If ground control points (GCPs) are available, they can be added here and included in the bundle adjustment. The Ori-RPC-deg1 file is created as an output from the previous step.

Code

```
mm3d Campari "(.*).tif" Ori-RPC-d0 RPC-d0-adj
```

f. **DSM creation:** There are 2 options for DSM generation. One uses the Malt UrbanMNE command whereby the computation is carried out in the so-called terrain geometry, where the optimization is defined in the (X, Y) of the object space, to find the most optimal Z-coordinates. This geometry is well adapted to 2.5D surface computation. The other method uses the Malt GeoImage command which performs a Multiview matching in image geometry and subsequent fusion. (E. Rupnik 2021.) This is said to offer superior resulting DSMs than the former, but for this analysis, the former is done. This is due to certain complications encountered while running the latter analysis.

Code

```
mm3d Malt UrbanMNE .*.TIF Ori-RPC-d0-adj SzW=2 Regul=0.2
DoOrtho=1 NbVI=2 EZA=1
```

g. Georeferencing of the final output DSM is not done automatically but has to be applied manually by the analyst. For this paper, this step was done in ArcGIS Pro using the GeoLand official Salzburg orthophoto, available in ArcGIS Pro as a basemap. CRS is WGS 84 Psuedo-Mercator (WKID 3857) same as the reference Lidar.
h. Visualization of the output is done in ArcGIS Pro since the software itself lacks a GUI.

Finally, post-processing such as alignment, comparison, and clipping is done in ArcGIS Pro.

4. RESULTS

4.1. Compare Results from Agisoft and Micmac with Lidar Reference

To achieve relatively similar results, both Agisoft and Micmac analysis was done in the highest possible settings and output DSM was derived at 1m resolution.

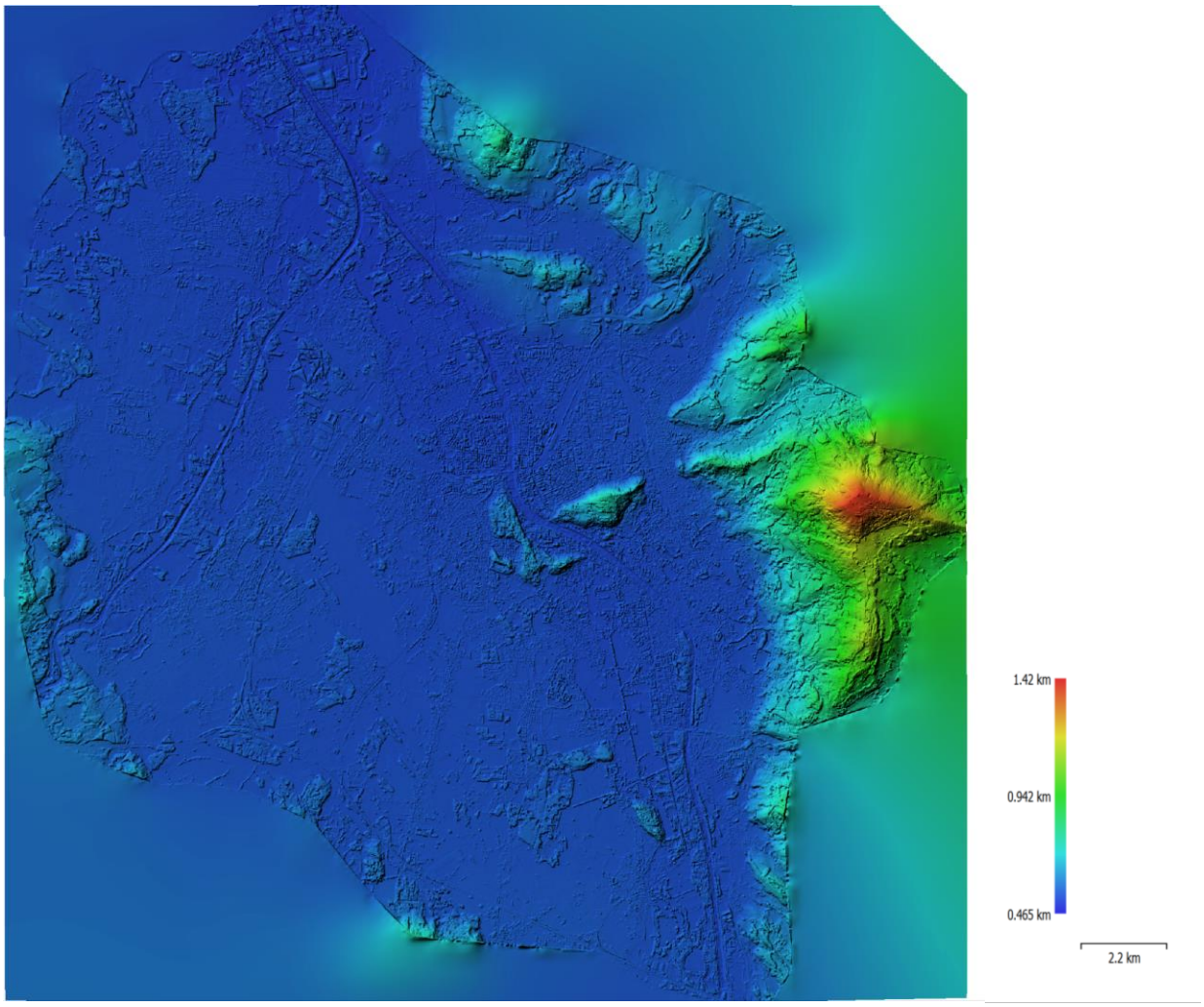

Figure 14. Output DSM for Salzburg from Agisoft

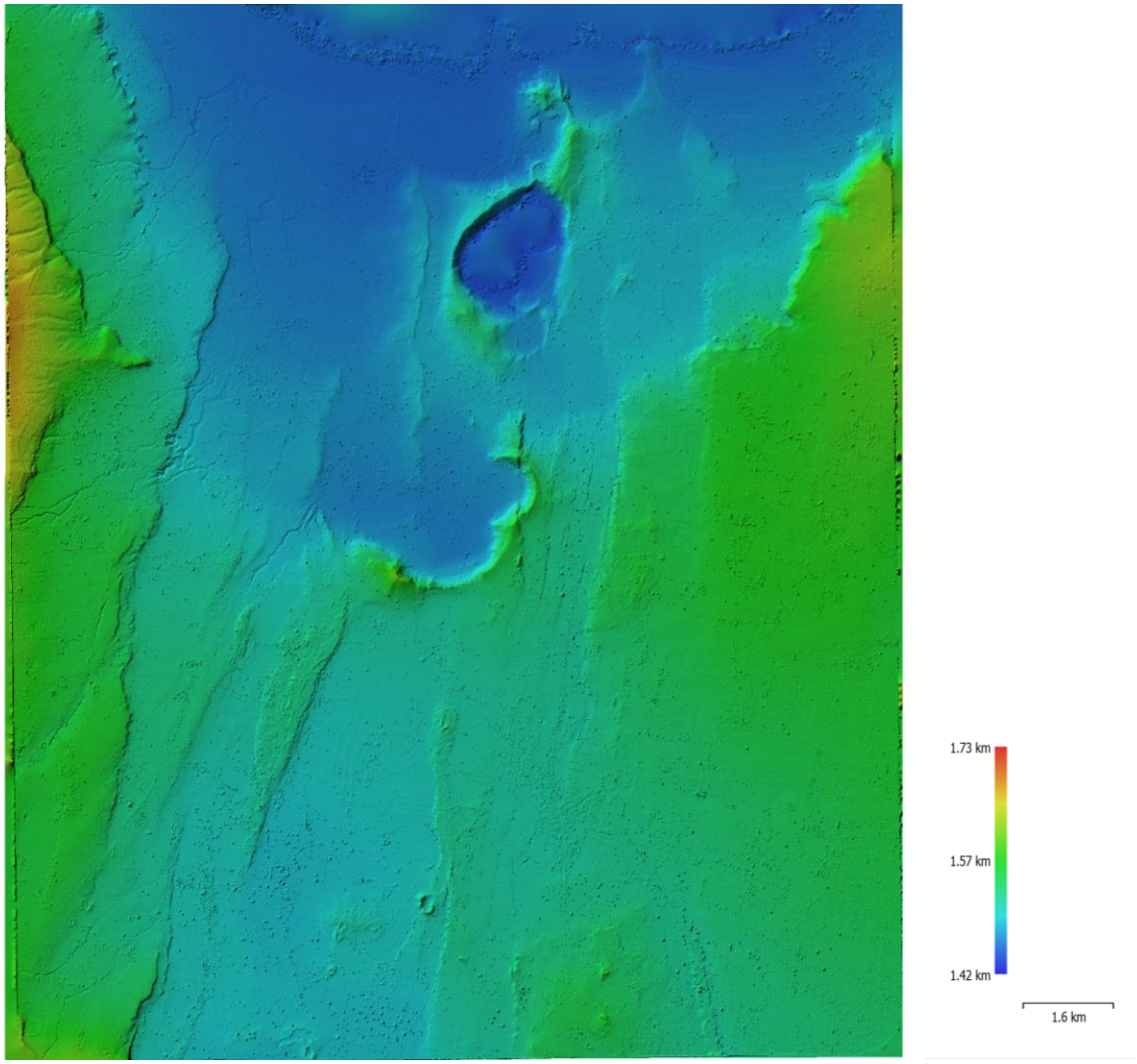

Figure 15. Output DSM for Shalla Lake, Ethiopia from Agisoft

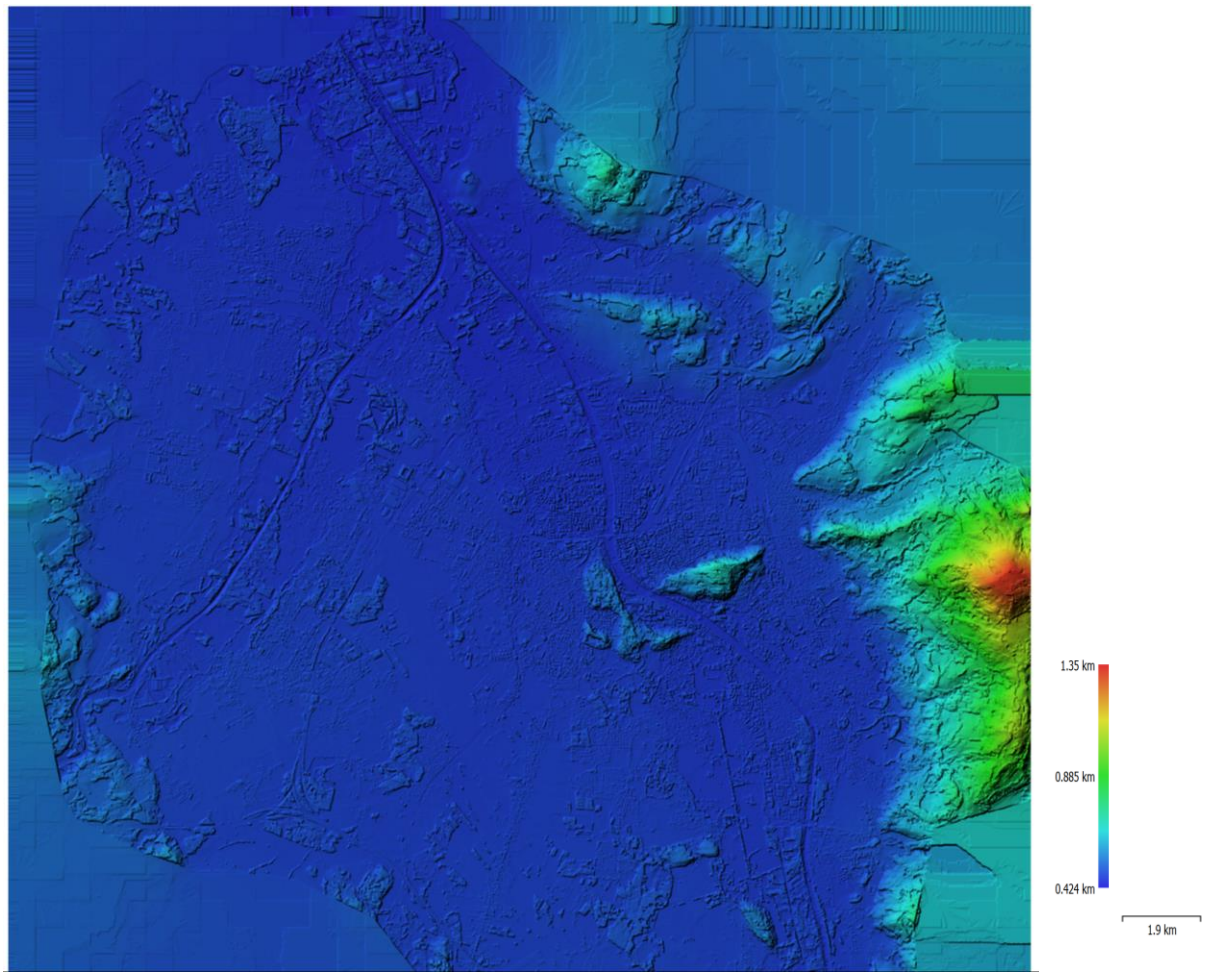

Figure 16. Output DSM after georeferencing and clipping to the extent of Salzburg from Micmac.

4.2. Vertical and Horizontal Accuracy

Points	Source	X value (°,')	Y value (°,')	Z value (m)
HBF	Lidar DSM	478128.65	136454.27	435
	Agisoft	474846.90	130243.55	542
	MicMac	474844.64	130245.92	479.95
Extreme North	Lidar DSM	477618.88	129744.13	436
	Agisoft	474856.05	125920.29	544.03
	MicMac	474857.28	125917.55	468.22
Rail Station	Lidar DSM	478167.44	130455.59	420
	Agisoft	474900.82	130244.05	529.55
	MicMac	474858.44	130246.67	472.30

Table 2. List of selected points and their corresponding values

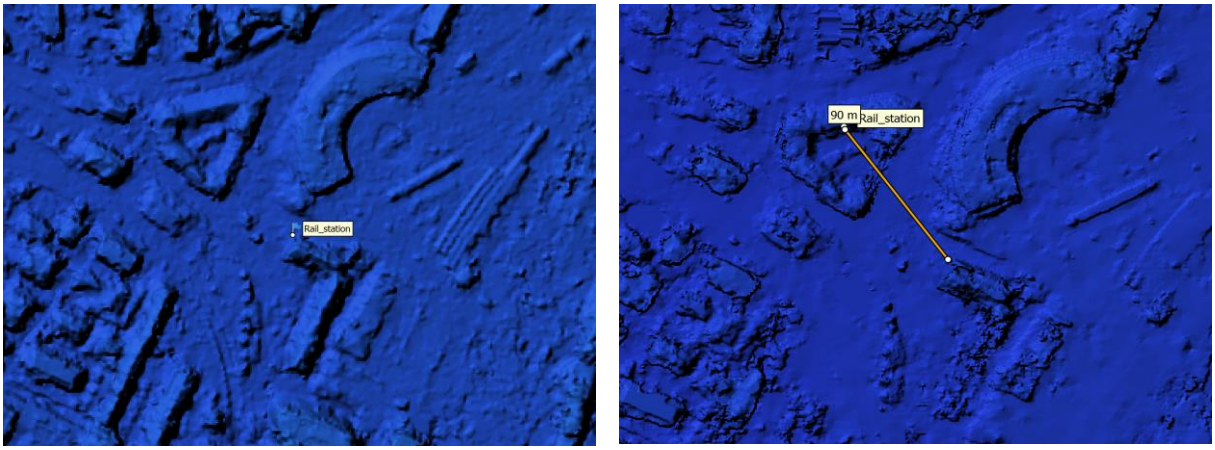

Figure 17. A point on Agisoft output(left) and on Micmac output(right) shows a 90m offset

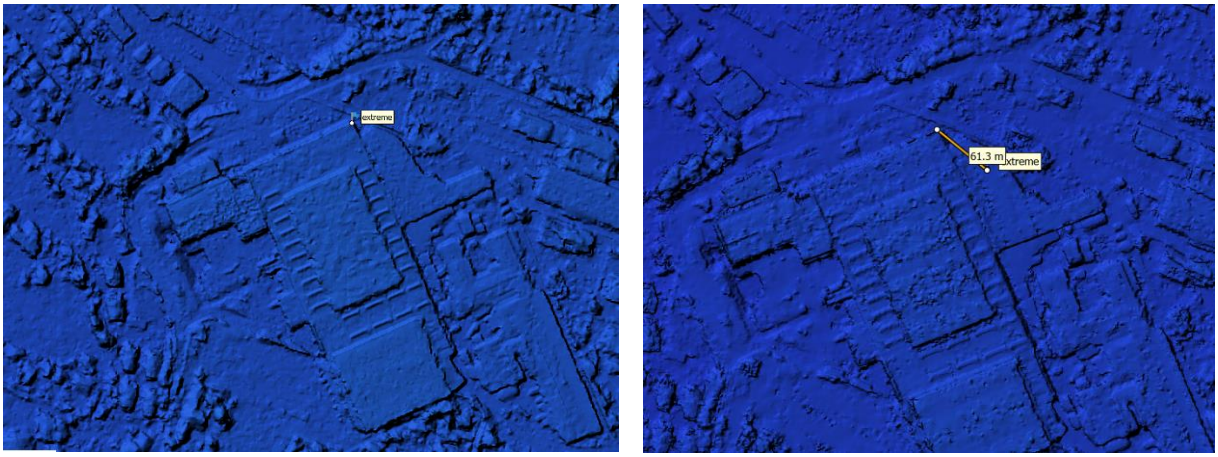

Figure 18. A point on Agisoft output(left) and on Micmac output(right) shows a 61m offset

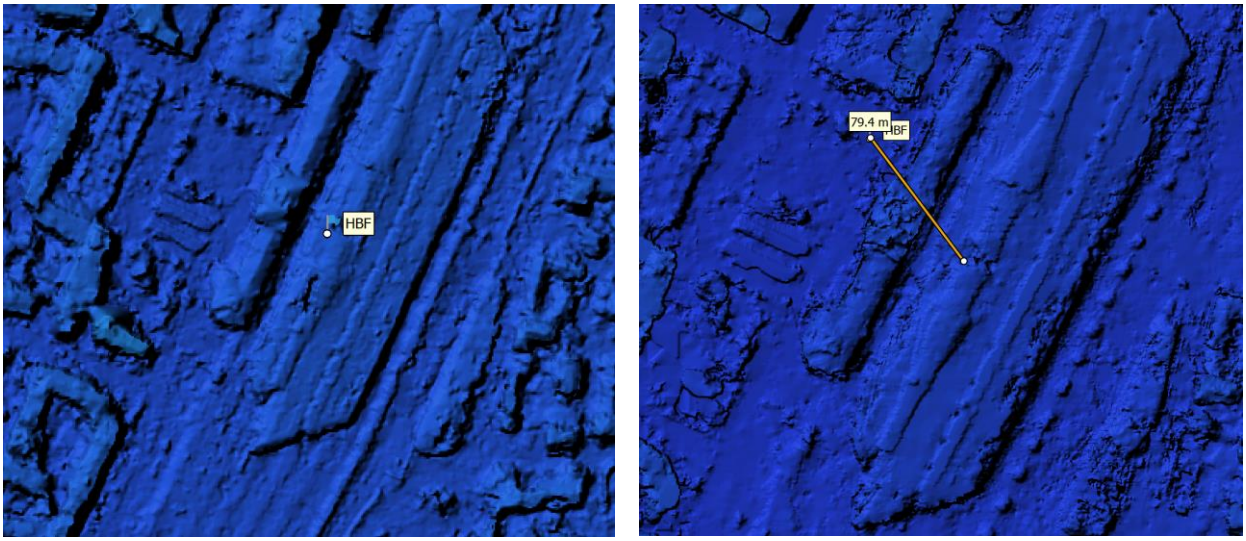

Figure 19. A point on Agisoft output(left) and on Micmac output(right) shows a 79.4m offset

Also, from the above, we see that the Agisoft output is much less noisy than the Micmac output. However, they cannot be compared to the lidar-derived DSM. See below.

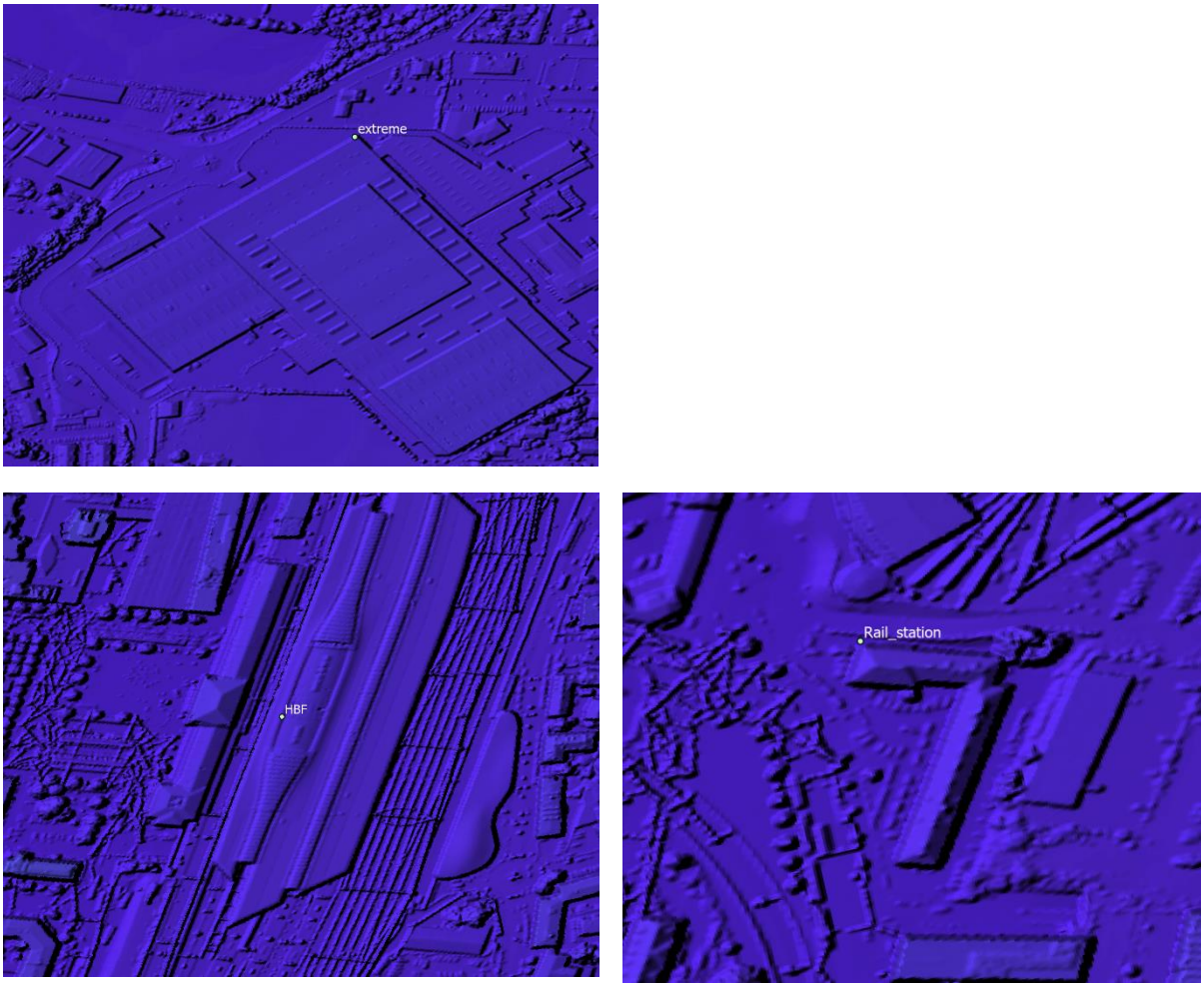

Figure 20 The three points on the Lidar-derived DSM.

4.3. RSME for Z (height) values

Root Mean Square Error (RMSE) is a statistical measure used to quantify the average difference between predicted values from a statistical model and the actual observed values. It provides a measure of accuracy, with lower values indicating better performance of the model or estimator in fitting the data. The formula is given as;

RSME = √(Σ [(predicted value - observed value)^2] / N)

For Agisoft

$$RMSE = \sqrt{((435-542)^2 + (420-529)^2 + (436-544)^2 / 3)}$$

$$RMSE = 108$$

For Micmac

$$RMSE = \sqrt{((435-477)^2 + (420-472)^2 + (436-468)^2 / 3)}$$

$$RMSE = 48$$

4.4. 1D Flood Model Testing

To test out the performance of the created DSMs in a flood model, a simple 1D flood model (unsteady flow simulation) using arbitrary flow information, was created in HEC RAS 6.4.1 for which each of the created DSMs were used as underlying terrain. The model was not adjusted to account for terrain-specific variations. This step is meant to evaluate if the difference in DSM vertical or horizontal accuracy has an obvious effect on the flood model's simulation. It does not aim to evaluate the accuracy of the flood model itself.

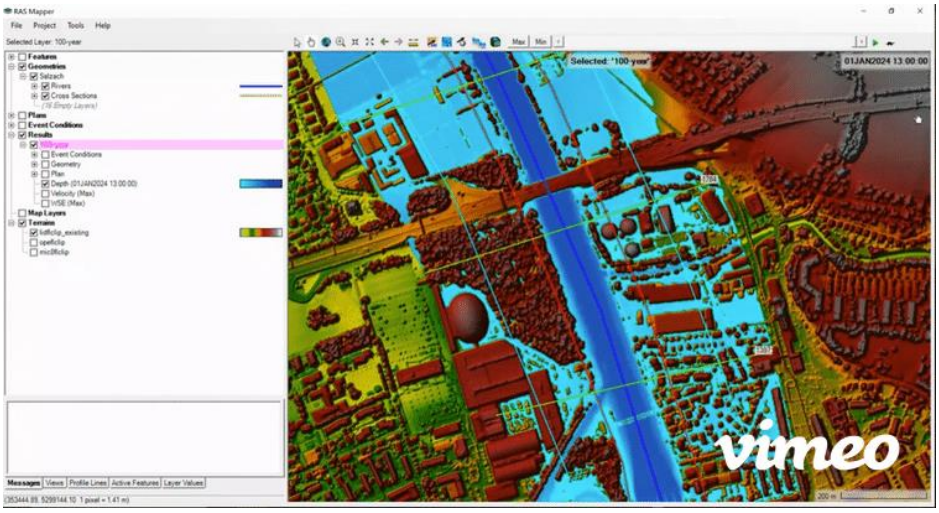

GIF video of the DSMs performance in a 1D flood model.

liflclip_existing is the lidar-derived DSM, opeflclip is the Agisoft-created DSM and micflclip being is the MicMac-created DSM. Please click **here** for a longer video.

5. DISCUSSION

The high RSM of 108m and 46m vertical offset for Agisoft and MicMac outputs respectively shows a significant deviation from actual height values for the Agisoft workflow. Also, significant horizontal offsets are observed in the Agisoft products as illustrated in Figures 17 to 20. Using accurate and sufficient GCP points in the Bundle adjustment may be used to improve this.

Also, while bundle adjustment is done for the MicMac workflow, it is just a basic one done without accurate GCPs. However, the improvements noticed in the vertical and horizontal accuracy may be a result of the manual georeferencing process done after the DSM had already been created.

The significant horizontal offset of the Agisoft DSM is also clearly visible in the flood simulation. The vertical offset however does not seem to affect the model's flow. This may be due to certain parameters which need to be further tuned to take the terrain into better consideration.

Software Comparison in Terms of Efficiency and Usability

Properties	**Agisoft Metashape**	**MicMac**
GUI	Yes	No
Processing Time	reasonable	poor
Progress tracking	Yes	No
Forum/Community	Helpful	Somewhat helpful
Beginner Friendly	Yes	Hard No

Table 3.

6. CONCLUSION

This paper has sought to test DSM creation using a Stereo Photogrammetry workflow and currently existing open-source (MicMac) and proprietary (Agisoft Metashape) photogrammetry software, with provided Tri-stereo satellite imagery. The aim was to evaluate the outputs from these softwares, by comparing them in terms of horizontal and vertical accuracy (relative to reference similar resolution Lidar derived DSM), usability, and efficiency.

The results showed that while neither the Agisoft nor MicMac-created DSMs can be ranked equally with the lidar-derived DSM in terms of noise, vertical and horizontal accuracy, the MicMac DSM fared better than Agisoft in terms of horizontal and vertical accuracy alone (with a height RMSE of 48m against Micmac's 108m), while the Agisoft DSM performed better than MicMac in terms of noise. This is mostly attributable to the fact that georeferencing for the MicMac product was done manually.

Also, in terms of usability and ease of use, Agisoft exceeds Micmac significantly due to its straightforward workflows and GUI, documentation, and an online forum where questions can be asked and answered promptly. However, the major downside is the fact that the algorithms running in the backend are not always clearly explained, and parametrization is sometimes not flexible.

Micmac however is not beginner friendly. The processing timelines are also significantly higher than average with a process on a large high-resolution imagery taking as much as 24 hours. Progress tracking is also nonexistent so upon starting a processing step, the user has no idea how long it may take. Lastly, the documentation is not very explanatory and the software has a steep learning curve.

REFERENCES

Bodoque, J. M., Aroca-Jiménez, E., Eguibar, M., & García, J. A. (2023). Developing reliable urban flood hazard mapping from LiDAR data. *Journal of Hydrology*, *617*. https://doi.org/10.1016/j.jhydrol.2022.128975

Gong Ke, & Fritsch Dieter. (2019). DSM Generation from High Resolution Multi-View Stereo Satellite Imagery. *Photogrammetric Engineering and Remote Sensing*.

Palaseanu-Lovejoy, M., Bisson, M., Spinetti, C., Buongiorno, M. F., Alexandrov, O., & Cecere, T. (2019). High-resolution and accurate topography reconstruction of Mount Etna from Pleiades satellite data. *Remote Sensing*, *11*(24). https://doi.org/10.3390/rs11242983

Reinstaller, S., Krebs, G., Pichler, M., & Muschalla, D. (2022). Identification of High - Impact Uncertainty Sources for Urban Flood Models in Hillside Peri - Urban Catchments. *Water (Switzerland)*, *14*(12). https://doi.org/10.3390/w14121973

Riedler, B., Bäuerl, M., Wendt, L., Kulessa, K., & Öze, A. (2017). Remote-Sensing Applications to Support Rehabilitation of Water Infrastructure in Lapilang, Nepal. *GI_Forum*, *1*, 183–198. https://doi.org/10.1553/giscience2017_01_s183

Yang, L., Meng, X., & Zhang, X. (2011). SRTM DEM and its application advances. In *International Journal of Remote Sensing* (Vol. 32, Issue 14, pp. 3875–3896). Taylor and Francis Ltd. https://doi.org/10.1080/01431161003786016